C. R. Mecanique 345 (2017) 678–689

Contents lists available at ScienceDirect

Comptes Rendus Mecanique

www.sciencedirect.com

A novel method based on maximum likelihood estimation for the construction of seismic fragility curves using numerical simulations

Cong-Thuat Dang [a], Thien-Phu Le [b,*], Pascal Ray [c]

[a] The University of Danang – University of Science and Technology, 54 Nguyen Luong Bang, Danang, Viet Nam
[b] LMEE, Université d'Évry Val-d'Essonne, 40, rue du Pelvoux, 91020 Évry cedex, France
[c] École nationale supérieure des mines de Saint-Étienne, 158, cours Fauriel, 42023 Saint-Étienne cedex 02, France

ARTICLE INFO

Article history:
Received 28 January 2017
Accepted 29 June 2017
Available online 1 August 2017

Keywords:
Seismic fragility curve
Numerical simulation
Maximum likelihood estimation
Log normal probability law
Peak ground acceleration
Damage state

ABSTRACT

Seismic fragility curves presenting some probability of failure or of a damage state exceedance versus seismic intensity can be established by engineering judgment, empirical or numerical approaches. This paper focuses on the latter issue. In recent studies, three popular methods based on numerical simulations, comprising scaled seismic intensity, maximum likelihood estimation and probabilistic seismic demand/capacity models, have been studied and compared. The results obtained show that the maximum likelihood estimation (MLE) method is in general better than other ones. However, previous publications also indicated the dependence of the MLE method on the ground excitation input. The objective of this paper is thus to propose a novel method improving the existing MLE one. Improvements are based on probabilistic ground motion information, which is taken into account in the proposed procedure. The validity of this new approach is verified by analytical tests and numerical examples.

1. Introduction

A seismic fragility curve expresses the probability of failure or damage of a structure or a mechanical system due to earthquakes as a function of a ground motion index; for instance, peak ground acceleration (PGA), peak ground velocity (PGV), spectral acceleration at a period of interest (PS_a), and so on. It is one of three ingredients, comprising seismic hazard, fragility curves and dominant accident sequences, which lead to core damage in a plant in the context of a probabilistic risk assessment (PRA) in nuclear engineering application [1,2]. Fragility curves are also applied to different structural types in the civil engineering field, e.g., buildings [3,4], bridges [5–11], special structures: chimneys [12], piping systems [13], tunnels [14], highway and railway embankments and cuts [15], etc. They are useful for the design of a new structure, and for an existing one they are helpful for seismic retrofitting decisions, disaster response planning, and quick loss estimation [5,6].

Depending on the source of data, fragility curves can be obtained either by (i) engineering judgment, (ii) an empirical approach or (iii) numerical simulation. This paper focuses on the construction of seismic fragility curves using numerical simulations in which three components are necessary: (i) methods to generate ground motion histories of a site, (ii) methods

* Corresponding author.
E-mail addresses: dangcongthuat@dut.udn.vn (C.-T. Dang), thienphu.le@univ-evry.fr (T.-P. Le), pascal.ray@mines-stetienne.fr (P. Ray).

http://dx.doi.org/10.1016/j.crme.2017.06.011

to simulate dynamic (in general non-linear) responses and verify damages states, and (iii) methods to derive fragility curves from obtained data. This study is situated in the third component, where there are three popular methods: (i) scaled seismic intensity (SSI), (ii) maximum likelihood estimation (MLE), and (iii) probabilistic seismic demand model/probabilistic seismic capacity model (PSDM/PSCM).

In a recent comparative publication, Mandal et al. [16,17] showed that the MLE method provides the most accurate [16] and very good [17] fragility estimations when comparing the MLE method with the "conventional" method and the PSDM/PSCM method (called "regression method" by the authors) via a test case concerning the primary containment dome of a typical Indian Pressurized Heavy Water Reactor (PHWR). Twenty-four ground motions records were used and fragility curves were verified with the discrete results of failure probability obtained by the Incremental Dynamic Analysis (IDA).

Lallement et al. [18] studied three methods for the construction of fragility curves: the method of moments (MM), a method minimizing the weighted sum of squared error (SSE) that is similar to the SSI method, and the MLE method in infill frame buildings. Based on the damage survey data of the January 12, 2010 earthquake in Haiti, and the data of simulation in an eight-story infill frame building using the IDA technique, the authors concluded that the MLE method is preferable to both the MM and SSE methods. A twenty-two far-field ground motion set was used for simulation data, and derived fragility curves were compared with analytical IDA results.

It should be noted that, in most of the previous works, a limited number of ground motion records of similar seismological origins were scaled to discrete values of seismic intensity, and they were then used for the IDA and the construction of fragility curves. However, Grigoriou [19] reported a difference of probabilistic distribution between the original ground motion index and its scaled version. The scaling technique for ground motions is not recommended.

Without the scaling technique, Dang [20] and Le et al. [21] used the Boore's model [22] to generate ground motions, and compared SSI, MLE and PSDM/PSCM methods on linear/non-linear oscillators and non-linear frame structures. The accuracy of the obtained fragility curves was checked with the results of the Monte-Carlo Simulation (MCS) method. The authors arrived to the same conclusion: the MLE method is the best in most of the considered cases. However, the MLE method suffers a shortcoming relative to ground motion time histories selected for simulations. Zentner [23] and Gehl et al. [24] indicated that fragility estimates are best when the ground acceleration histories are close to the median capacity level, so there is a good chance of obtaining failure as well as non-failure cases. If no failure case is observed, the MLE method might not converge. This fact highlighted that the construction procedure of a fragility curve depends on the choice of ground acceleration histories, although the fragility curve is considered as intrinsic to the structure. For a given site, the chosen acceleration histories must be consistent and their ground motion index (PGA for instance) must follow the probability distribution relative to the site. Therefore, the observed data (failure or non-failure) that were used for constructing fragility curves also depend on the probability distribution of the ground motion index. In the existing MLE method, this dependence is however not explicit.

The aim of this paper is thus to propose a novel method by improving the existing MLE method. The basic idea is to incorporate in the maximum likelihood estimation stage both response information and also excitation information via the probability distribution of the ground motion index, which is absent in the MLE method. The proposed method is thus called "Excitation and Response-based Maximum Likelihood Estimation" (ERMLE) method. The development of the ERMLE method in section 2 is preceded by a background about fragility curve definitions and a summary of the MLE method in the form of a step-by-step procedure. Theoretical formulations of the ERMLE method are then deployed via a step-by-step procedure for practical applications. Two comparison criteria are also proposed in order to verify the efficiency of the proposed method. Analytical tests and numerical examples are used in section 3 to validate the ERMLE method. Finally, conclusions are given in section 4.

2. Seismic fragility curves

2.1. Definitions

Let A be a chosen ground motion index, also called an "intensity measure" (IM). A can be PGA, PGV, PS_a and so on. The fragility curve $F_r(a)$ is the conditioned probability of failure or of exceeding a damage state given that $A = a$:

$$F_r(a) = P[X \geq x_0 | A = a] \tag{1}$$

where the failure or the specific damage state is characterized when the structural response X exceeds a critical limit x_0. Taking into account random properties of response and critical limits due to uncertainty in loadings, material properties, dimensions and so on, the failure or the specific damage state can be considered in a more general way as the excess by seismic demand D of the seismic capacity C. The definition of the fragility curve thus becomes

$$F_r(a) = P[D \geq C | A = a] \tag{2}$$

Once the fragility curve $F_r(a)$ is available, using the distribution of the ground motion index A of a site, it is possible to calculate the probability of failure or damage state of the site by using the integral

$$p_f = \int_{-\infty}^{+\infty} F_r(a)\, p_A(a)\, \mathrm{d}a = \int_{0}^{+\infty} F_r(a)\, p_A(a)\, \mathrm{d}a \tag{3}$$

where $p_A(a)$ is the probability distribution of index A for the considered site. In general, A is positive, which is why the integral bounds are limited from zero to infinity in Eq. (3). A commonly accepted assumption for a fragility curve is that $F_r(.)$ is a cumulative distribution function of the log-normal law:

$$F_r(a; A_\mathrm{m}, \beta) = \Phi\left[\frac{\ln(a/A_\mathrm{m})}{\beta}\right] \tag{4}$$

where $\Phi(.)$ is the standard Gaussian cumulative distribution function, while A_m and β are respectively the median and logarithmic standard deviations. The log-normal assumption given in Eq. (4) greatly simplifies the original problem defined in Eq. (1) or Eq. (2). All existing methods now lead to the determination of two parameters: A_m and β.

Note that the fragility curve defined in Eq. (4) is also called "composite" fragility curve because it does not distinguish random uncertainties (inherent, not reducible uncertainties) and epistemic uncertainties (uncertainties due to lack of knowledge). For the composite fragility curve, the median capacity A_m is related to inherent random phenomena (random uncertainties), while the logarithmic standard deviation β is associated with both random and epistemic uncertainties [23].

2.2. Existing MLE method

In the Maximum Likelihood Estimation (MLE) method [25–27], the basic idea is to associate the failure or the damage state event with a Bernoulli random variable Y. The use of MLE to identify the distribution of Y leads to a fragility curve. The step-by-step procedure is as follows:

– step 1: generate or choose a set of N independent ground accelerations $a_i(t)$, $i = 1 \dots N$. Their values of ground motion index are computed from $a_i(t)$ and equal to a_i;

– step 2: simulate structural responses subjected to the ground accelerations $a_i(t)$ and verify whether the failure or the damage state is reached. Consider a Bernoulli random variable Y; if $a_i(t)$ gives rise to failure or damage, Y is given the value $y_i = 1$; otherwise, $y_i = 0$;

– step 3: formulate the likelihood function $L(A_\mathrm{m}, \beta)$

$$L(A_\mathrm{m}, \beta) = \prod_{i=1}^{N} [F_r(a_i; A_\mathrm{m}, \beta)]^{y_i} [1 - F_r(a_i; A_\mathrm{m}, \beta)]^{1-y_i} \tag{5}$$

– step 4: identify A_m and β from the optimization problem below

$$(\hat{A}_m, \hat{\beta}) = \arg\min_{A_\mathrm{m}, \beta} (-L(A_\mathrm{m}, \beta)) \tag{6}$$

As previously analyzed in section 1, the data used for the MLE method are N couples (a_i, y_i), where a_i are values of the ground motion index, calculated from the chosen ground accelerations $a_i(t)$ for a given site. The ground motion index A is random and therefore it must follow a probability distribution of the site. The data (failure or non-failure) depends thus not only on the behavior of structure via its fragility curves, but also on the choice of ground accelerations in Step 1. However, the likelihood function modeling this data given in Eq. (5) does not take into account in an explicit way the distribution of A for the site. We propose in the following section a new formulation of the likelihood function to take explicitly into account the probability distribution of the ground motion index A.

2.3. New method based on maximum likelihood estimation

Let $p_{A|\Omega_\mathrm{f}}(a)$ and $p_{A|\Omega_\mathrm{s}}(a)$ represent the conditional probability density functions of the ground motion index A, given that the structure is respectively in the failure domain Ω_f and the safety domain Ω_s:

$$p_{A|\Omega_\mathrm{f}}(a) = p_A(a|D \geq C) \quad \text{and} \tag{7}$$

$$p_{A|\Omega_\mathrm{s}}(a) = p_A(a|D < C) \tag{8}$$

Using Bayes' rule for two random events "$A = a$" and failure "$D \geq C$", the conditional probability density can be calculated by

$$p_{A|\Omega_\mathrm{f}}(a) = p_A(a|D \geq C) = \frac{p_A(a) P[D \geq C|A = a]}{\int_0^{+\infty} p_A(a) P[D \geq C|A = a]\, \mathrm{d}a} \tag{9}$$

where $p_A(a)$ is probability density function of the seismic intensity A. Note that $P[D \geq C|A = a]$ is the definition of the fragility curve $F_r(a)$ in Eq. (2) and the integral formula in the denominator of Eq. (9) is in fact the failure probability p_f in Eq. (3). Equation (9) thus becomes

$$p_{A|\Omega_f}(a) = \frac{p_A(a)F_r(a)}{\int_0^{+\infty} p_A(a)F_r(a)\,\mathrm{d}a} = \frac{p_A(a)F_r(a)}{p_f} \tag{10}$$

A similar analysis leads to the conditional density probability of A in the safety domain $p_{A|\Omega_s}$ by the following formula

$$p_{A|\Omega_s}(a) = \frac{p_A(a)\,(1-F_r(a))}{\int_0^{+\infty} p_A(a)\,(1-F_r(a))\,\mathrm{d}a} = \frac{p_A(a)\,(1-F_r(a))}{1-p_f} \tag{11}$$

The knowledge of distributions $p_A(a)$, $p_{A|\Omega_s}(a)$ and $p_{A|\Omega_f}(a)$ enables us to deduce the fragility curve $F_r(a)$.

If only failure domain data are used, the likelihood function to maximize is

$$L(A_m,\beta) = \prod_{i=1}^{N_f}\left[p_{A|\Omega_f}(a_i)\right] = \prod_{i=1}^{N_f}\left[\frac{F_r(a_i;A_m,\beta)p_A(a_i)}{\int_0^{+\infty} F_r(a;A_m,\beta)p_A(a)\,\mathrm{d}a}\right] \tag{12}$$

where N_f is the number of accelerations giving the failure of the structure.

If only safety domain data are used, the likelihood function to maximize is

$$L(A_m,\beta) = \prod_{i=1}^{N_s}\left[p_{A|\Omega_s}(a_i)\right] = \prod_{i=1}^{N_s}\left[\frac{(1-F_r(a_i;A_m,\beta))p_A(a_i)}{1-\int_0^{+\infty} F_r(a;A_m,\beta)p_A(a)\,\mathrm{d}a}\right] \tag{13}$$

where N_s is the number of accelerations giving the safety of the structure.

If all the data, including failure and safety cases, are used, the likelihood function to maximize is

$$\begin{aligned} L(A_m,\beta) &= \prod_{i=1}^{N}\left[p_{A|\Omega_f}(a_i)\right]^{y_i}\left[p_{A|\Omega_s}(a_i)\right]^{1-y_i} \\ &= \prod_{i=1}^{N}\left[\frac{F_r(a_i;A_m,\beta)p_A(a_i)}{\int_0^{+\infty} F_r(a;A_m,\beta)p_A(a)\,\mathrm{d}a}\right]^{y_i}\left[\frac{(1-F_r(a_i;A_m,\beta))p_A(a_i)}{1-\int_0^{+\infty} F_r(a;A_m,\beta)p_A(a)\,\mathrm{d}a}\right]^{1-y_i} \end{aligned} \tag{14}$$

where $N = N_s + N_f$ is the total number of accelerations and $y_i = 1$ for the failure case and $y_i = 0$ otherwise. Theoretically, with $N_s \to +\infty$ and $N_f \to +\infty$, the likelihood functions given in Eqs. (12), (13) and (14) lead to the same results of parameters (A_m, β). However, in real situations, data are limited and numerical simulations of the mechanical problem are time consuming, it is therefore preferred to use the whole data, as indicated in Eq. (14)

The full procedure of this novel method, called 'Excitation and Response-based Maximum Likelihood Estimation' and abbreviated as 'ERMLE', is described in the following step-by-step process.

– Step 0: estimate the probability density function of the ground motion index $p_A(a)$. There are following possibilities:

- $p_A(a)$ is already available thanks to previous studies or experts' judgment, for example;
- $p_A(a)$ is not available and it is to elaborate from ground motion histories. A large set of ground motion histories is recommended for an accurate estimation of $p_A(a)$:
  - if the distribution law of $p_A(a)$ is available, for instance a log-normal distribution, the parameters of $p_A(a)$ can be easily determined by a parametric method for example: maximum likelihood-based method or moments-based method;
  - if the distribution law of $p_A(a)$ is not available, $p_A(a)$ can be deduced by using a non-parametric method such as the kernel method from ground motion histories.

– Step 1: generate or choose a set of N independent ground accelerations $a_i(t)$, $i = 1 \ldots N$. Their values of ground motion index are computed from $a_i(t)$ and equal to a_i. If PGA is chosen as the ground motion index, then $\mathrm{PGA}_i = a_i = \max_t |a_i(t)|$.

– Step 2: simulate structural responses subjected to the ground accelerations $a_i(t)$ and verify whether the failure or damage state is reached. Consider a Bernoulli random variable Y; if $a_i(t)$ gives rise to the failure or damage state, Y takes a value $y_i = 1$; otherwise $y_i = 0$.

– Step 3: formulate the likelihood function $L(A_m, \beta)$ given in Eq. (14) using the whole data set. The integral in the denominator of Equation (14) is calculated numerically.

– Step 4: Identify A_m and β from the optimization problem indicated in Eq. (6).

Note that the numbers of ground motion histories in Step 0 and in Steps 1 and 2 are not necessarily equal. In general, a high number of ground motion histories in Step 0 is used because it is not time consuming, whereas a lesser number of ground motion histories is used in Steps 1 and 2 because the computation of Step 2 is much heavier.

In comparison with the existing method in section 2.2 where the failure event is considered as a Bernoulli random variable, the proposed method is based on the conditional probability distributions of the ground motion index A: $p_{A|\Omega_f}(a_i)$ and $p_{A|\Omega_s}(a_i)$. The obtained failure events in the MLE method depend not only on mechanical systems but also on the choice of limited ground accelerations that are used for mechanical simulations. That implies the dependence of fragility curves on the choice of ground motions as reported in references [23,24]. For the proposed ERMLE method, the step 0 is added to take into account the distribution of the ground motion index A and then, it is incorporated in the likelihood functions. This addition of distribution A is expected to reduce the dependence of fragility curves on the choice of the ground motions in step 1 because each a_i in Eqs. (12), (13) and (14) can be seen as weighted by $p_A(a_i)$.

2.4. Comparison criteria

In order to compare the effectiveness of the proposed method applied to numerical examples, it is necessary to propose some comparison criteria. Using the results of the Monte Carlo simulation method as a reference, the first criterion is based on the distance between a fragility curve and the reference results. This criterion is called the Mean Square Error (MSE) and defined as:

$$\mathrm{MSE} = \frac{1}{N_I}\sum_{j=1}^{N_I}\left[F_r^{\mathrm{X}}(a_j) - F_r^{\mathrm{MCS}}(a_j)\right]^2 \tag{15}$$

where $F_r^{\mathrm{X}}(a)$ is the curve obtained from the ERMLE or MLE methods, while $F_r^{\mathrm{MCS}}(\cdot)$ is the result obtained by the Monte Carlo simulation method, which is described just below. N_I is the number of narrow intervals a_j of ground motion index A. The higher the MSE value of a fragility curve, the farther it is from the Monte Carlo results.

The second criterion concerns the use of a fragility curve for the estimation of failure probability using Eq. (3). It is the Relative ERror (RER) between the failure probability estimated by the ERMLE or MLE methods p_f^{X} and that given by the Monte Carlo simulation method p_f^{MCS}:

$$\mathrm{RER} = \frac{\left|p_f^{\mathrm{X}} - p_f^{\mathrm{MCS}}\right|}{p_f^{\mathrm{MCS}}} \times 100\% \tag{16}$$

where p_f^{X} is obtained from $F_r^{\mathrm{X}}(a)$ and the probability density function $p_A(a)$ by:

$$p_f^{\mathrm{X}} = \int_0^{+\infty} F_r^{\mathrm{X}}(a)\, p_A(a)\, \mathrm{d}a \tag{17}$$

$F_r^{\mathrm{MCS}}(.)$ in Eq. (15), and p_f^{MCS} in Eq. (16), are computed from the Monte Carlo simulation method with the following step-by-step procedure:

– Step 1: Generate or choose a large number N_{MCS} of independent ground accelerations $a_i(t)$, $i = 1 \ldots N_{\mathrm{MCS}}$. Their corresponding values of ground motion index are calculated from the ground accelerations and equal to a_i.

– Step 2: Organize these ground accelerations with respect to their interval of ground motion index $a_i \in [a_j - \mathrm{d}a, a_j + \mathrm{d}a]$. There are thus N_I intervals, and in an interval j there are N_j ground accelerations. Note that $N_{\mathrm{MCS}} = \sum_{j=1}^{N_I} N_j$.

– Step 3: Simulate seismic responses subjected to the ground accelerations $a_i(t)$ and check the failure or damage state of the structure.

– Step 4: Estimate $F_r^{\mathrm{MCS}}(.)$ and p_f^{MCS}:

$$F_r^{\mathrm{MCS}}(a_j) \cong \frac{\sum_{i}^{N_j} \mathbf{1}\left[D \geq C | A = a_i \in \left[a_j - \mathrm{d}a, a_j + \mathrm{d}a\right]\right]}{N_j},\ j = 1 \ldots N_I \tag{18}$$

$$p_f^{\mathrm{MCS}} \cong \frac{\sum_{i}^{\mathrm{MCS}} \mathbf{1}\left[D \geq C | A = a_i\right]}{N_{\mathrm{MCS}}} \tag{19}$$

where $\mathbf{1}[.]$ is the indicator function, equal to 1 if the failure or damage state is reached and equal to 0 otherwise.

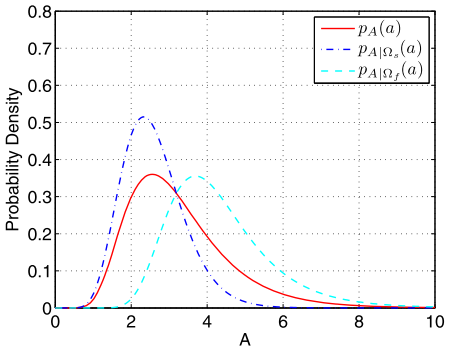

Fig. 1. Illustration of the probability density functions.

In the procedure of the Monte Carlo simulation method, we propose to fix the total number of ground accelerations N_{MCS} and the half-length of intervals da. In general, a high number N_{MCS} should be chosen to insure the convergence of the Monte Carlo simulation method. A trade-off of da should be made in order to obtain a good approximation of $F_r^{\mathrm{MCS}}(a_j)$ from ground accelerations in intervals $[a_j - \mathrm{d}a, a_j + \mathrm{d}a]$. The interval d$a$ should be small enough to get the narrow intervals, but da should also be large enough to a have sufficient number of ground accelerations in these intervals.

Note that the Monte Carlo simulation method is used here as a reference and that it is not used in practice because its computational cost is very high.

3. Validation

3.1. Analytical tests

The objectives of these tests are double: (i) to verify the accuracy of the conditional probability distributions in Eqs. (10) and (11), the foundation of the ERMLE method and (ii) to check the identification capacity of its proposed procedure when data are perfectly known.

To reach these objectives, we suppose that the seismic hazard $p_A(a)$ and the fragility curve $F_r(a)$ are analytically known. This allows us to generate a set of N samples of A based on $p_A(a)$, and then separate them into two subsets, failure and safety, based on $F_r(a)$ by drawing a uniform random variable U in interval $[0, 1]$. If $u_i \leq F_r(a_i)$, then a_i is in the failure subset; otherwise a_i is in the safety subset. From N_{f} samples a_i of the failure subset and N_{s} samples a_i of the safety subset, it is possible to compare with the formulae of $p_{A|\Omega_{\mathrm{f}}}(a)$ in Eq. (10) and $p_{A|\Omega_{\mathrm{s}}}(a)$ in Eq. (11). It is also possible to identify fragility curve parameters and compare them with exact values.

3.1.1. Verification of $p_{A|\Omega_{\mathrm{f}}}(a)$ and $p_{A|\Omega_{\mathrm{s}}}(a)$

It was assumed that the seismic index A followed the log-normal distribution $p_A \equiv p_{LN}(a; 3.0, 0.4)$ and the fragility curve was $F_r(a) \equiv F_{LN}(a; 3.5, 0.3)$ where $p_{LN}(a; A_{\mathrm{m}}, \beta)$ is defined as

$$p_{LN}(a; A_{\mathrm{m}}, \beta) = \frac{1}{a\beta\sqrt{2\pi}} \exp\left[-\frac{(\ln(a/A_{\mathrm{m}}))^2}{2\beta^2}\right] \tag{20}$$

and $F_{LN}(a; A_{\mathrm{m}}, \beta)$ is its cumulative distribution function. Based on the above definition of $p_{LN}(\cdot)$ and $F_{LN}(\cdot)$, the units of A_{m} and β are respectively unit A and the natural log of unit A. For example, if A is PGA measured in g, the units of A_{m} and β are respectively g and ln(g).

First, from the formulae in Eqs. (10), (11), the probability density functions $p_{A|\Omega_{\mathrm{f}}}(a)$ and $p_{A|\Omega_{\mathrm{s}}}(a)$ were obtained, and are shown in Fig. 1 together with $p_A(a)$.

Then a set of $N = 5000$ samples of A: a_i, $i = 1 \ldots N$ was generated with the distribution function $p_A(a)$. Using the known fragility curve $F_r(a)$, the initial set of A was then divided into two subsets: N_{f} samples in the failure case and N_{s} in the safety case. Note that $N = N_{\mathrm{f}} + N_{\mathrm{s}}$. Using N_{f} failure samples and N_{s} safety samples, their histograms were plotted and the quantiles of sample data were estimated. Then these results were compared with the theoretical results of $p_{A|\Omega_{\mathrm{f}}}(a)$ in Eq. (10) and $p_{A|\Omega_{\mathrm{s}}}(a)$ in Eq. (11) obtained above.

Fig. 2 presents a comparison between the results of simulations with $N = 5000$ and theoretical results. It can be noted that the agreement is close to perfect and thus validates the formulation of $p_{A|\Omega_{\mathrm{f}}}(a)$ and $p_{A|\Omega_{\mathrm{s}}}(a)$ and the method for simulation data.

3.1.2. Identification of the fragility curve $F_r(a)$

A new example was considered with the distribution of A: $p_A \equiv p_{LN}(a; 3.0, 0.4)$ and the fragility curve: $F_r(a) \equiv F_{LN}(a; 7.0, 0.2)$. The probability of failure calculated with Eq. (3) gave $p_{\mathrm{f}} = 0.0291$. It means that there was a lesser chance

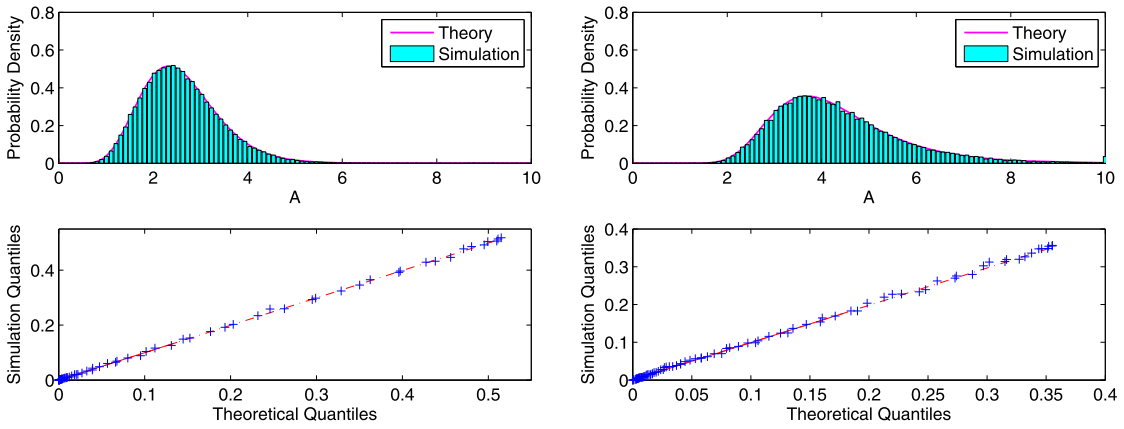

(a) Safety case (b) Failure case

Fig. 2. Validation of $p_{A|\Omega_f}(a)$ and $p_{A|\Omega_s}(a)$.

Table 1
Analytical test: selected data and identified fragility curves.

N_f	N_s	$\hat{p}_f$	MLE				ERMLE			
			$\hat{A}_m$	ϵ_{A_m} (%)	$\hat{\beta}$	ϵ_β (%)	$\hat{A}_m$	ϵ_{A_m} (%)	$\hat{\beta}$	ϵ_β (%)
60	10000	0.0060	8.78	25.4	0.239	19.8	7.03	0.5	0.202	1.3
120	10000	0.0119	7.99	14.2	0.228	14.3	7.05	0.7	0.208	4.2
180	10000	0.0177	7.52	7.5	0.217	8.5	7.04	0.6	0.206	3.4
240	10000	0.0234	7.21	2.9	0.203	1.5	7.04	0.6	0.199	0.1
300	10000	0.0291	7.01	0.2	0.198	0.7	7.05	0.8	0.199	0.3
360	10000	0.0347	6.84	2.16	0.190	4.7	7.04	0.6	0.194	2.8
420	10000	0.0403	6.72	3.9	0.185	7.0	7.04	0.6	0.191	4.0
480	10000	0.0458	6.62	5.3	0.181	9.2	7.03	0.5	0.188	5.5
540	10000	0.0512	6.53	6.5	0.182	8.7	7.02	0.4	0.191	4.3
600	10000	0.0566	6.47	7.5	0.182	8.9	7.05	0.8	0.193	3.5

($\approx 3\%$) of having failure events in simulations. Using the same simulation method as in the previous test, N samples a_i $(i = 1 \dots N)$ of A involving samples in the failure subset and samples in the safety subset were generated; they were used to identify the fragility curve parameters with those in the existing MLE method and in the proposed ERMLE method. In order to study the dependence of the identified results on the available data, N_s samples from the safety subset and N_f samples from the failure subset were randomly selected to be tested. The approximate probability of failure of this selected data is $\hat{p}_f = \dfrac{N_f}{N_s + N_f}$.

Table 1 presents the results for different data sets where N_s was fixed at 10000 samples and N_f varied from 60 to 600. The identified values $\hat{A}_m$ and $\hat{\beta}$ are compared with the exact ones, and the relative errors ϵ_{A_m} and ϵ_β are calculated.

Fig. 3 shows the relative errors in the identified parameters with respect to $\hat{p}_f$ using the MLE and ERMLE methods. We can note a better stability for the proposed ERMLE method than the MLE method, despite different ground motion sets.

3.2. Numerical examples

In order to test the efficiency of the proposed procedure in simulated data situations, the ERMLE and MLE methods were applied to numerical examples of linear and non-linear oscillators. The choice of simple-degree-of-freedom systems here seems simple, but it does not make us lose the generality of the methodology used in the ERMLE and MLE methods. In fact, for the step 2 of the procedures given in sections 2.2 and 2.3, the mechanical simulation component can be considered as a black box to obtain failure or not failure response for a ground acceleration history.

Time ground accelerations were generated using the stochastic method proposed on Boore's studies [22,28]. PGA was considered here as ground motion index and thus for each acceleration history $a_i(t)$, the PGA value a_i was its maximum absolute value in time. The fragility curves of each structure derived from a same set of time accelerations using the ERMLE and MLE methods were compared via the criteria given in section 2.4.

3.2.1. Ground motion histories

The stochastic method proposed by Boore [22] assumes that ground motion is distributed with random phase over a time duration related to earthquake size and propagation distance. The ground motion is characterized by its spectrum –

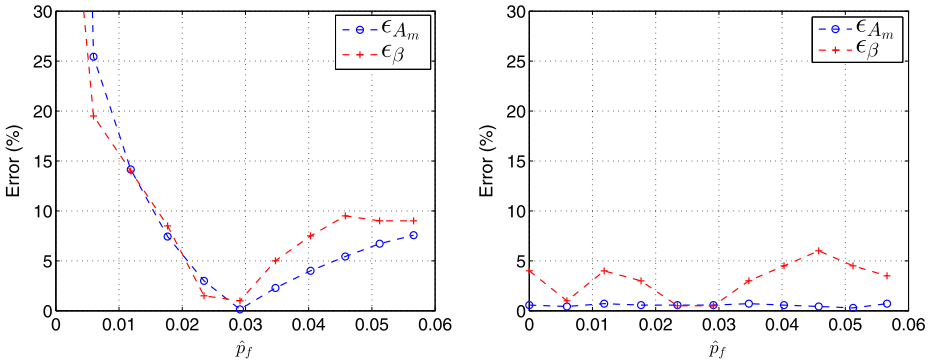

Fig. 3. Relative errors in the fragility curve parameters for different data sets.

this is where the physics of earthquake process and wave propagation are contained, usually encapsulated and put into the form of simple equations. The total spectrum of the motion at a site $S(M_0, R, f)$ is considered as a combination of the earthquake source (E), the path (P), the site (G), and the type of motion (I).

$$S(M_0, R, f) = E(M_0, f)P(R, f)G(f)I(f) \tag{21}$$

where M_0 is the seismic moment that is related to the seismic magnitude M by

$$M = \frac{2}{3}\log M_0 - 10.7 \tag{22}$$

R is the distance from the source to the site and f is the frequency. By separating the spectrum of ground motion into source, path, and site components, the models based on the stochastic method can be easily modified to account for specific situations or to account for improved information about particular aspects of the model.

Given the spectrum motion at a site, Boore [22] suggests the simulation of ground motions using six steps: (i) a white noise (Gaussian or uniform) is generated for a duration given by the duration of the motion; (ii) this noise is then windowed; (iii) the windowed noise is transformed into a frequency domain; (iv) the spectrum is normalized by the square-root of the mean square amplitude spectrum; (v) the normalized spectrum is multiplied by the ground motion spectrum $S(M_0, R, f)$; (vi) the resulting spectrum is transformed back to a time domain to obtain a time history of ground motions. This method for simulation of time series is implemented by Boore in Fortran [28].

In order to generate time acceleration series for the numerical examples, we implemented the stochastic method in Matlab software [29]. Parameters of the ground spectrum were taken as suggested values in reference [22] and summarized as indicated below:

– the source $E(M_0, f)$: is based on the source spectral shape AS00 (Atkinson and Silva (2000) for California);

– the path $P(R, f)$: takes into account the effects of geometrical spreading, of attenuation and of the increase of duration with distance due to wave propagation and scattering.

$$P(R, f) = Z(R)\exp\left(-\frac{\pi f R}{Q(f)c_Q}\right) \tag{23}$$

where $c_Q = 3.5$, $Q(f) = 180f^{0.45}$ and $Z(R)$ defined by

$$Z(R) = \begin{cases} \dfrac{R_0}{R} & \text{if} \quad R \le R_1 \\ Z(R_1)\left(\dfrac{R_1}{R}\right)^{p_1} & \text{if} \quad R \ge R_1 \end{cases} \tag{24}$$

with $R_0 = 1$, $R_1 = 40$ and $p_1 = 0.5$;

– the site $G(f)$: takes into account the effects due to the local site geology and is divided into amplification $A(f)$ and attenuation $D(f)$

$$G(f) = A(f)D(f) \tag{25}$$

where the amplification $A(f)$ is taken for generic rock in reference [30] and the attenuation function $D(f)$ is defined as the combination of two filters

$$D(f) = \left[1 + \left(\frac{f}{f_{\max}}\right)^8\right]^{-\frac{1}{2}} \quad \text{and} \quad D(f) = \exp(-\pi\kappa_0 f) \tag{26}$$

where $f_{\max} = 100$ Hz and $\kappa_0 = 0.03$;

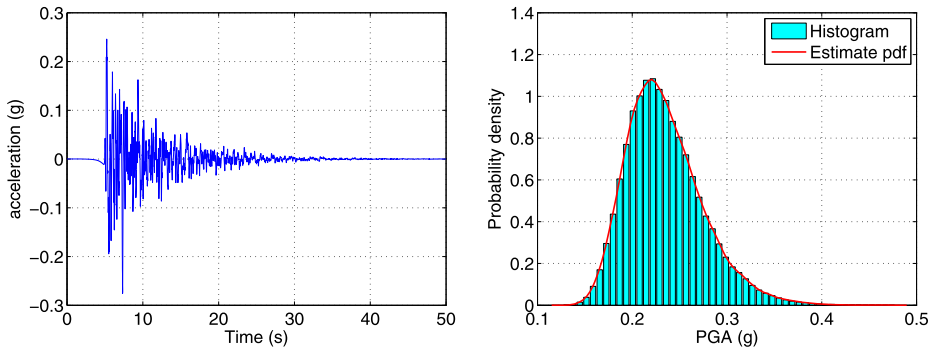

(a) Simulated ground acceleration (b) PGA distribution

Fig. 4. Boore's model with $M = 7$ and $R = 9$ km.

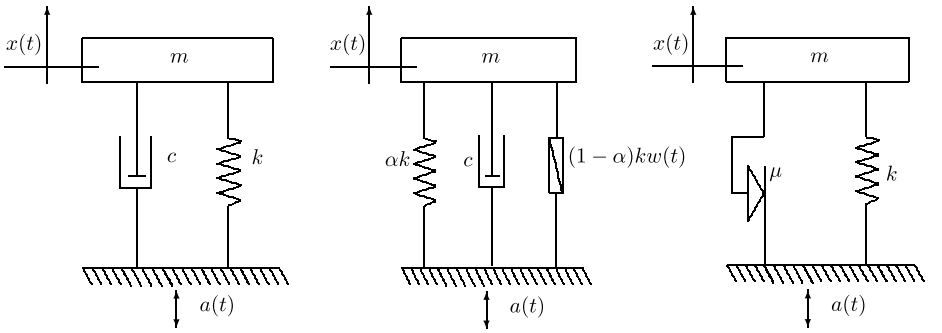

Fig. 5. Linear (left), Bouc–Wen (middle) and Coulomb (right) oscillators.

– the motion type $I(f)$ for acceleration is defined as

$$I(f) = -(2\pi f)^2 \tag{27}$$

Fig. 4(a) shows an acceleration time series of the model for magnitude $M = 7$ and $R = 9$ km. Using 2×10^5 accelerations with the same magnitude and distance, a probability density function of PGA can be obtained by the kernel method and is indicated in Fig. 4(b).

3.2.2. Oscillators

Two oscillators (linear and Bouc–Wen non-linear) used in reference [31] and a Coulomb non-linear oscillator were considered here.

$$\underline{\text{Linear}} : \ddot{x}(t) + 2\zeta\omega_0\dot{x}(t) + \omega_0^2 x(t) = -a(t) \tag{28}$$

$$\underline{\text{Bouc–Wen}} : \ddot{x}(t) + 2\zeta\omega_0\dot{x}(t) + \omega_0^2(\alpha x(t) + (1-\alpha)w(t)) = -a(t) \tag{29}$$

$$\text{avec } \dot{w}(t) = C_1\dot{x}(t) - C_2\,|\dot{x}(t)|\,|w(t)|^{n_d-1}\,w(t) - C_3\dot{x}(t)\,|w(t)|^{n_d}$$

$$\underline{\text{Coulomb}} : \ddot{x}(t) + \mu g\,\text{Sgn}\,(\dot{x}(t)) + \omega_0^2 x(t) = -a(t) \tag{30}$$

where ω_0 (rad/s) is the natural angular frequency; ζ is the damping ratio; for Bouc–Wen behavior, $w(t)$ is hysteretic displacement and α, C_1, C_2, C_3, n_d are constants; for the Coulomb model, μ is the damping friction coefficient, $a(t)$ is the ground acceleration and g is the gravitational acceleration. Fig. 5 shows the three models. Numerical values of parameters were inspired by Kafali and Grigoriu [31]: $\omega_0 = 5.9$ rad/s, $\zeta = 2\%$ for the linear oscillator; $C_1 = 1$, $C_2 = C_3 = 0.5$ cm^{n_d}, $\alpha = 0.1$, $n_d = 1$ for the Bouc–Wen oscillator; $\mu = 0.01$ and $g = 9.81$ m/s^2 for the Coulomb oscillator.

Fig. 6 shows an illustration of the oscillators' responses under a seismic excitation that were obtained with the Runge–Kutta algorithm in Matlab software [29].

The failure of an oscillator was verified by comparing displacement $x(t)$ with a displacement limit x_0, i.e. in the definition of Eq. (2): $D = \max_t |x(t)|$ and $C = x_0$. Thus, if $D \geq C \Leftrightarrow \max_t |x(t)| \geq x_0$, the failure or damage state was reached, and if $D < C \Leftrightarrow \max_t |x(t)| < x_0$, it was not attained. A displacement limit $x_0 = 13$ cm was chosen corresponding to the case of $p_f < 10\%$, i.e. failure events much less than safety events.

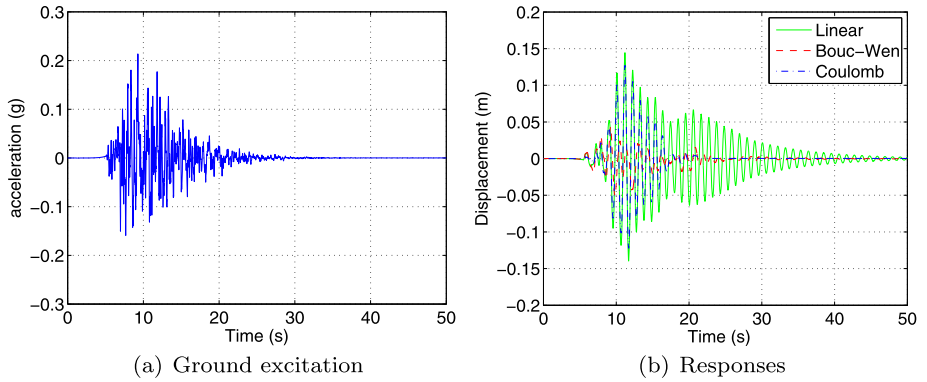

Fig. 6. Illustration of the oscillator's responses under a ground acceleration.

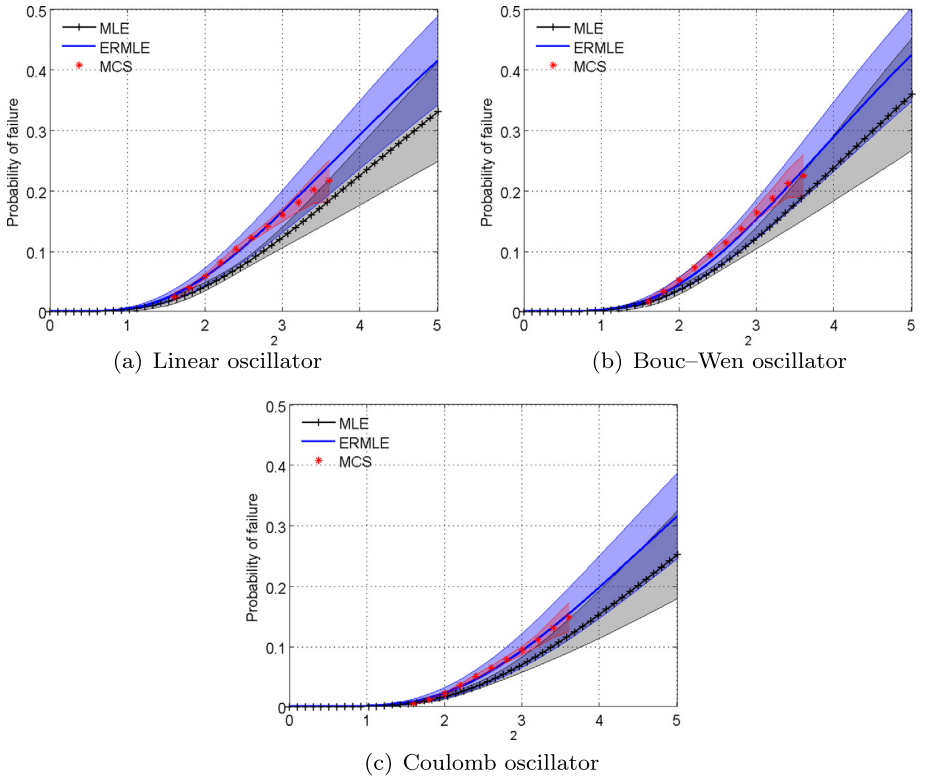

Fig. 7. Mean fragility curves and 95% confidence intervals in shaded zones: gray (MLE), blue (ERMLE), red (MCS).

Using $N = 5000$ ground accelerations generated from the Boore model ($M = 7$, $R = 9$ km) and the responses of the corresponding oscillators, fragility curves obtained by the MLE and ERMLE methods were computed. In order to investigate the statistical characteristics of these fragility curves, the bootstrap resampling technique with replacement was applied [23]. From original data comprising simulated results obtained with 5000 ground accelerations, 1000 new samples, each of size 5000 were built by random sampling with replacement. Each bootstrap sample allowed an estimate of parameters (A_{m} and β) and thus a sample of fragility curve. The mean fragility curve and the 95% confidence interval were then deduced based on 1000 fragility curves of the 1000 bootstrap samples. Fig. 7 presents the mean fragility curves and the 95% confidence intervals for the linear, Bouc–Wen and Coulomb oscillators.

Note that the Monte Carlo Simulation method (MCS) was also performed with a greater number of ground accelerations: $N = 2 \times 10^5$. These accelerations were organized into $N_I = 11$ PGA intervals a_j: $[a_j - 0.1; a_j + 0.1]$ m/s^2. The MCS results are represented in Fig. 7 by plus sign markers (+) together with the bounds of the 95% confidence interval. The probabilities of failure $\hat{p}_f$ estimated by the MCS are also given in Table 2. It can be noted from Fig. 7 that the fragility curves of the two methods are well separated and the MCS results are closer to the ERMLE fragility curves than to those of the MLE method.

Table 2
Oscillators: results of comparison criteria.

Oscillator	$\hat{p}_f$	MLE		ERMLE	
	MCS	MSE $\times 10^{-3}$	RER%	MSE $\times 10^{-3}$	RER%
Linear	0.097	0.81	28.05	0.22	1.68
Bouc–Wen	0.090	0.93	28.18	0.07	9.53
Coulomb	0.049	0.39	28.15	0.01	3.51

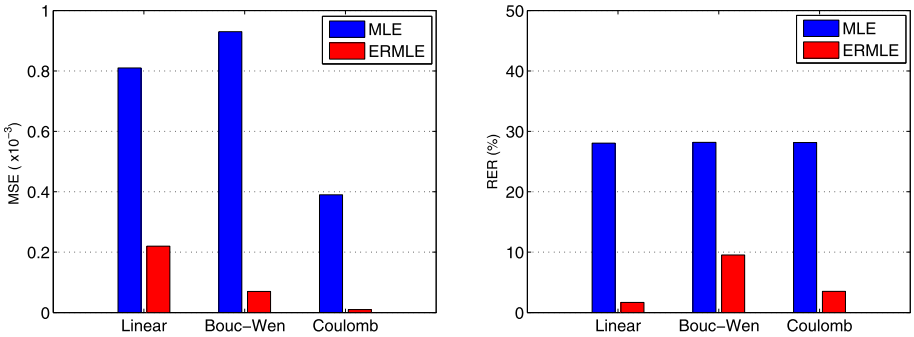

Fig. 8. Oscillators: Discrepancy with respect to MCS results.

Moreover, the MLE fragility curves are always outside of the 95% confidence intervals of the MCS method, while the ERMLE fragility curves are inside or very close.

Using the two comparison criteria in section 2.4, MSE and RER were calculated and they are given in Table 2 and plotted in Fig. 8.

Once again, the proposed ERMLE method is much better than the MLE method when comparing MSE and RER values.

4. Conclusions

A fragility curve is an important tool for seismic probabilistic risk assessment, and the Maximum Likelihood Estimation (MLE) method is an efficient method for its construction via numerical simulations. However, the MLE method presents a disadvantage relative to the dependence of ground motions, particularly when failure events are rare, such as the low failure probability in a seismic situation. The objective of this paper has been to propose a novel method called the "Excitation Response-based Maximum Likelihood Estimation" (ERMLE) method to overcome this drawback. Note that the scaling technique for ground motions was excluded from this study because it modifies artificially the probability distribution of PGA [19].

In the ERMLE method, probabilistic excitation information is taken into account. It is readily obtained either from seismic hazard data provided by an earth scientist or from a large number of ground motion simulations. In combining excitation information and fragility curve properties, the conditional probabilities, given the failure or the safety of the ground motion index, are deduced and are used to establish the likelihood functions. The solution to the maximum likelihood problem provides the fragility curve parameters. The presence of $p_A(a)$ in the likelihood functions allows one to reduce the dependence of the derived fragility curves on the chosen sets of ground motions. Of course, it demands an additional task of a numerical integral calculation. The ERMLE method is implemented in practical use by a step-by-step procedure.

The validation of the proposed method was performed by analytical tests and numerical examples. In the first case, the fragility curve was assumed to be perfectly known and the tests aimed to (i) verify the conditional probabilities of the ground motion index, given failure or safety conditions, i.e. the foundation of the ERMLE method, and (ii) retrieve the original fragility curve with the MLE and ERMLE methods. An excellent agreement of the conditional probabilities was obtained between the exact formula and the simulation. The ERMLE proved to be more efficient and less sensitive than the existing MLE method when data were not complete and failure data were not numerous.

The ERMLE and MLE methods were then applied to examples of linear and non-linear oscillators. The precision of each method was checked in comparison with results of the Monte-Carlo method with a high number of simulations. The critical limit $x_0 = 13$ cm is chosen to simulate a difficult situation when failure events are rarer than safety events ($p_f \leq 10\%$). The obtained results indicate that the ERMLE method is superior to the MLE one.

The validation and verification performed on analytical tests and numerical examples of oscillators show clearly that the ERMLE method represents an improvement of the existing MLE method when the available data are not complete or failure data are rare. More complex structural models and real structures should be tested in the next step of this study, but the similar conclusion would be expected because in the ERMLE and MLE methods, the step of mechanical simulations can be considered as a black box to obtain a binary result: failure or not failure of the structure under a ground motion excitation.

References

[1] B.R. Ellingwood, Validation studies of seismic PRAs, Nucl. Eng. Des. 123 (1990) 189–196.
[2] R.P. Kennedy, C.A. Cornell, R.D. Campbell, S. Kaplan, H.F. Perla, Probabilistic seismic safety study of an existing nuclear power plant, Nucl. Eng. Des. 59 (2) (1980) 315–338.
[3] Y.J. Park, A.H.S. Ang, Y.K. Wen, Seismic damage analysis of reinforced concrete buildings, J. Struct. Eng. 111 (4) (1985) 740–757.
[4] B.R. Ellingwood, Earthquake risk assessment of building structures, Reliab. Eng. Syst. Saf. 74 (3) (2001) 251–262.
[5] K.R. Karim, F. Yamazaki, Effect of earthquake ground motions on fragility curves of highway bridge piers based on numerical simulation, Earthq. Eng. Struct. Dyn. 30 (12) (2001) 1839–1856.
[6] K.R. Karim, F. Yamazaki, A simplified method of constructing fragility curves for highway bridges, Earthq. Eng. Struct. Dyn. 32 (10) (2003) 1603–1626.
[7] S.H. Kim, M. Shinozuka, Development of fragility curves of bridges retrofitted by column jacketing, Probab. Eng. Mech. 19 (1–2) (2004) 105–112.
[8] K.R. Karim, F. Yamazaki, Effect of isolation on fragility curves of highway bridges based on simplified approach, Soil Dyn. Earthq. Eng. 27 (2007) 414–426.
[9] J.E. Padgett, R. DesRoches, Methodology for the development of analytical fragility curves for retrofitted bridges, Earthq. Eng. Struct. Dyn. 37 (8) (2008) 1157–1174.
[10] D.H. Tavares, J.E. Padgett, P. Paultre, Fragility curves of typical as-built highway bridges in Eastern Canada, Eng. Struct. 40 (2012) 107–118.
[11] K. Ramanathan, J.E. Padgett, R. DesRoches, Temporal evolution of seismic fragility curves for concrete box-girder bridges in California, Eng. Struct. 97 (2015) 1–12.
[12] C. Zhou, X. Zeng, Q. Pan, B. Liu, Seismic fragility assessment of a tall reinforced concrete chimney, Struct. Des. Tall Spec. Build. 24 (2015) 440–460.
[13] B.S. Ju, A. Gupta, Seismic fragility of threaded tee-joint connections in piping systems, Int. J. Press. Vessels Piping 132–133 (2015) 106–118.
[14] S.A. Argyroudis, K.D. Pitilakis, Seismic fragility curves of shallow tunnels in alluvial deposits, Soil Dyn. Earthq. Eng. 35 (2012) 1–12.
[15] S. Argyroudis, A.M. Kaynia, Analytical seismic fragility functions for highway and railway embankments and cuts, Earthq. Eng. Struct. Dyn. 44 (2015) 1863–1879.
[16] T.K. Mandal, N.N. Pujari, S. Ghosh, A comparative study of seismic fragility estimates using different numerical methods, in: 4th ECCOMAS Thematic Conference on Computational Methods in Structural Dynamics and Earthquake Engineering, 2013.
[17] T.K. Mandal, S. Ghosh, N.N. Pujari, Seismic fragility analysis of a typical Indian PHWR containment: comparison of fragility models, Struct. Saf. 58 (2016) 11–19.
[18] D. Lallemant, A. Kiremidjian, H. Burton, Statistical procedures for developing earthquake damage fragility curves, Earthq. Eng. Struct. Dyn. 44 (2015) 1373–1389.
[19] M. Grigoriu, To scale or not to scale seismic ground-acceleration records, J. Eng. Mech. 137 (4) (2010) 284.
[20] C.-T. Dang, Méthodes de construction des courbes de fragilité sismique par simulations numériques (in French), PhD thesis, Université Blaise Pascal, Clermont II, 2014.
[21] T.-P. Le, C.-T. Dang, P. Ray, A comparative study of construction methods for seismic fragility curves using numerical simulations, Mech. Ind. 17 (602) (2016).
[22] D.M. Boore, Simulation of ground motion using the stochastic method, Pure Appl. Geophys. 160 (3) (March 2003) 635–676.
[23] I. Zentner, Numerical computation of fragility curves for NPP equipment, Nucl. Eng. Des. 240 (6) (2010) 1614–1621.
[24] P. Gehl, J. Douglas, D. Seyedi, Influence of the number of dynamic analyses on the accuracy of structural response estimates, Earthq. Spectra 31 (1) (2015) 97–113, http://dx.doi.org/10.1193/102912EQS320M.
[25] M. Shinozuka, M. Feng, H. Kim, S. Kim, Nonlinear static procedure for fragility curve development, J. Eng. Mech. 126 (12) (2000) 1287–1295.
[26] M. Shinozuka, M. Feng, J. Lee, T. Naganuma, Statistical analysis of fragility curves, J. Eng. Mech. 126 (12) (2000) 1224–1231.
[27] M. Shinozuka, S.H. Kim, S. Kushiyama, J.H. Yi, Fragility curves of concrete bridges retrofitted by column jacketing, Earthq. Eng. Eng. Vib. 1 (2) (2002) 195–205.
[28] D.M. Boore, SMSIM Fortran programs for simulating ground motions from earthquakes, U.S. Geological Survey, 2005.
[29] MATLAB, version 7.9.0529 (R2009b), The MathWorks Inc., Natick, Massachusetts, 2009.
[30] D.M. Boore, W.B. Joyner, Site amplifications for generic rock sites, Bull. Seismol. Soc. Amer. 87 (1977) 327–341.
[31] C. Kafali, M. Grigoriu, Seismic fragility analysis: application to simple linear and nonlinear systems, Earthq. Eng. Struct. Dyn. 36 (2007) 1885–1900.